Supplementary information

Differentiation between bulk and interfacial properties: analysis of time-dependent carrier injection in perovskite solar cells

Naoyuki Nishimura[†]*, *Ranjan Kumar Behera*[†], *Daisuke Kubota*[§], *Hiroyuki Kanda*[†], *Kohei Yamamoto*[†], *Hiroyuki Yaguchi*[§], *Takurou N. Murakami*[†], *Hiroyuki Matsuzaki*[†]*

† National Institute of Advanced Industrial Science and Technology (AIST),1-1-1 Higashi, Tsukuba, Ibaraki 305-8565, Japan.

§ Graduate School of Science and Engineering, Saitama University, Saitama-shi, Saitama 338-8570, Japan

Corresponding Author

Naoyuki Nishimura, E-mail: naoyuki-nishimura@aist.go.jp

Hiroyuki Matsuzaki, E-mail: hiroyuki-matsuzaki@aist.go.jp

1. PV performance of PSCs before and after thermal stress

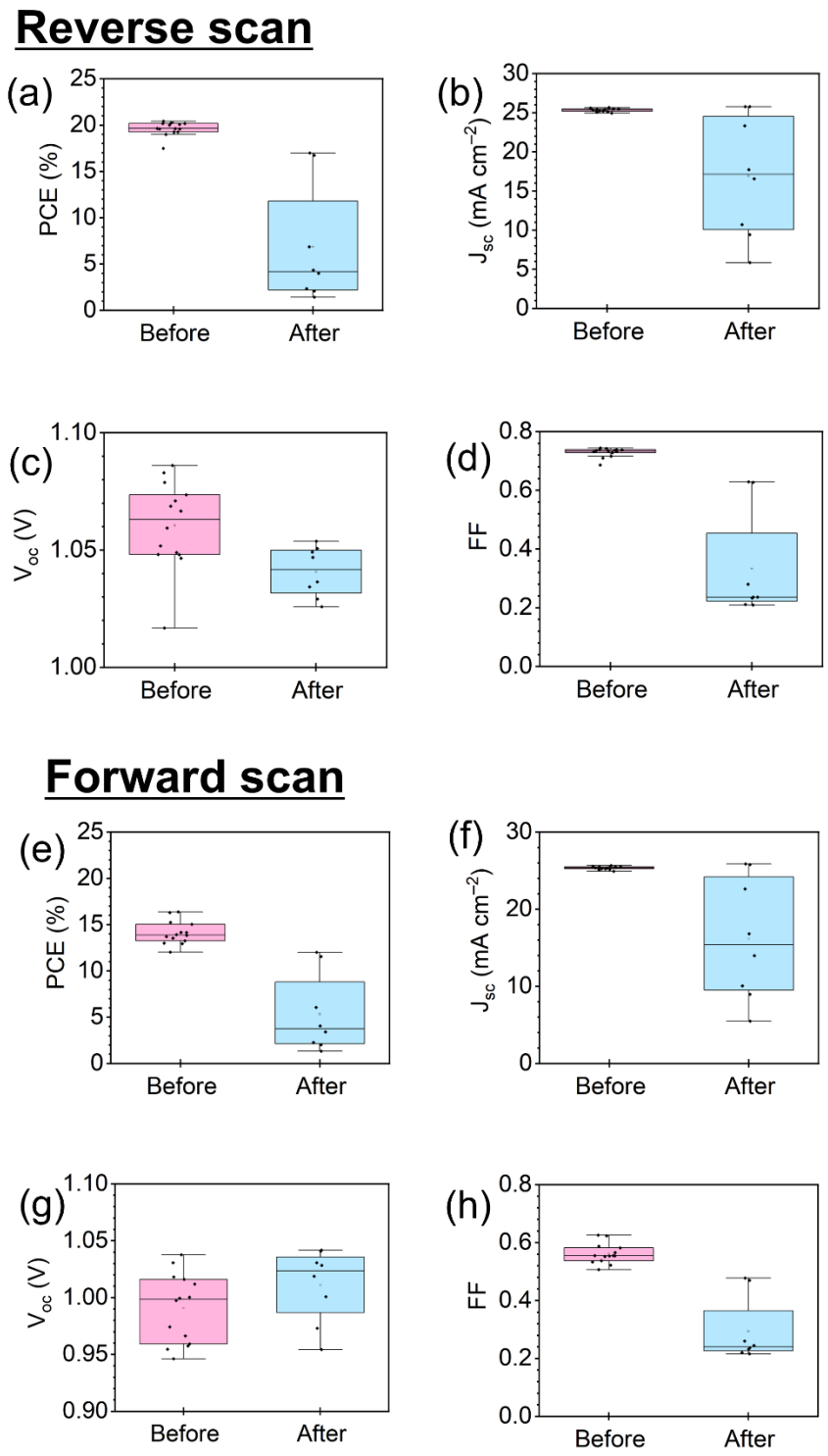

Fig. S1 PV parameters of PSCs before and after thermal stress at 358 K for 40 h; (a) PCE, (b) J_{sc}, (c) V_{oc}, and (d) *FF* in reverse scan; (e) PCE, (f) J_{sc}, (g) V_{oc}, and (h) *FF* in forward scan.

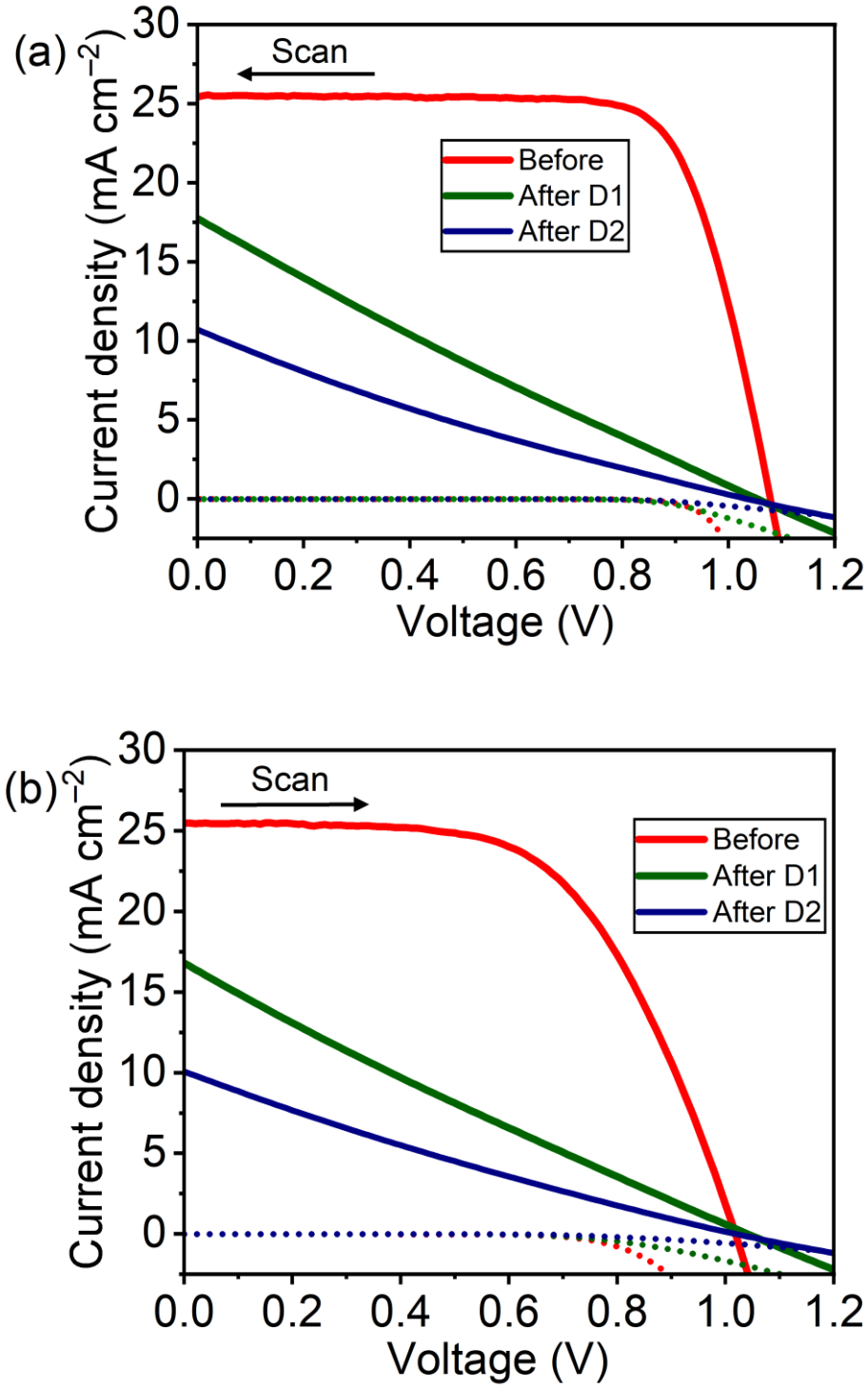

Fig. S2 J-V curves of PSCs before and after thermal stress (D1 and D2) corresponding to Table 1 (a) in reverse scan, (b) in forward scan.

Table S1. Averaged PV parameters of PSCs before and after thermal stress at 358 K for 40 h.

Sample	Scan	J_{sc} (mA/cm^2)	V_{oc} (V)	FF	PCE (%)
Before degradation	Reverse	25.3 ± 0.3	1.06 ± 0.2	0.73 ± 0.02	19.4 ± 1.0
	Forward	25.3 ± 0.2	0.98 ± 0.4	0.55 ± 0.04	13.8 ± 1.6
After degradation	Reverse	16.9 ± 7.2	1.04 ± 0.1	0.33 ± 0.17	6.8 ± 6.0
	Forward	16.2 ± 7.4	1.01 ± 0.3	0.29 ± 0.10	5.3 ± 4.0

The thermal stress reduced the magnitude of the hysteresis, as indicated by the increased hysteresis indexes ($PCE_{forward}/PCE_{reverse}$) from 75% to 93% for device D1, and up to 100% for device D2 (Table 1). Since the hysteresis typically originates from capacitive characters at the heterointerfaces, the observed reduction in the hysteresis after the thermal stress likely indicates improved heterointerface quality rather than deterioration. This interpretation is consistent with the findings obtained from the EPD-PLL measurements

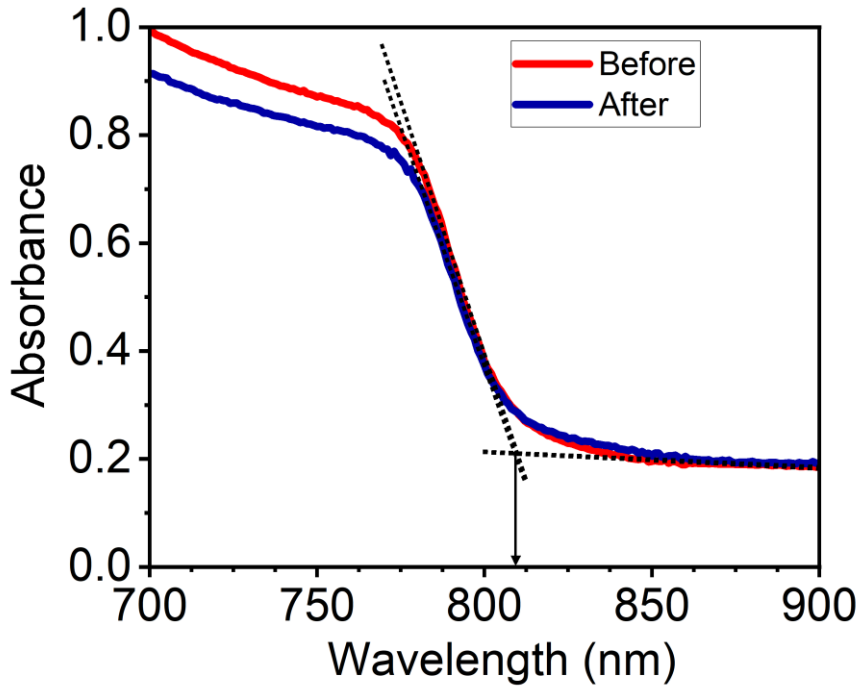

Fig. S3 Absorption spectra of perovskite monolayer films before and after thermal stress.

2. Analysis of EPD-PLL results for the perovskite monolayer sample

In the range of excitation power intensities under consideration here, the excitation power dependence of initial PL intensity and PL lifetime for the perovskite monolayer sample (Fig. S4) can be described by a simple rate equation that accounts for single-carrier trapping and/or recombination, as well as band-to-band radiative bimolecular (electron-hole) recombination. This can be expressed as follows[1, 2]:

$$\frac{dn}{dt} = -An - Bn^2, \qquad \text{(S1)}$$

$$I_{\mathrm{PL}} \propto Bn^2(t) + BNn(t) \qquad \text{(S2)}$$

Here, n and I_{PL} represent the photogenerated carrier density and the PL intensity, respectively. A, B, and N denote the rate constant for single-carrier trapping and/or recombination, the rate constant for band-to-band radiative bimolecular recombination, and the unintentional doped carrier density in the sample, respectively. The PL lifetime is defined as the time interval required for the initial PL intensity to decay to $1/e$ of its original value.

The initial photogenerated carrier density, n (t = 0) = n_0, at a fluence of 1 nJ/pulse is calculated to be 1.33×10^{15} cm^{-3}, based on the beam profile of the excitation light at the sample position and absorption coefficient (3.33×10^{4} cm^{-1}) [3] of the perovskite materials at 650 nm[3].

By solving the Equation S1 and applying relation S2, the time dependence of I_{PL} can be obtained as:

$$I_{PL}(t) = I_0\left(\frac{N}{N+n_0}\left(\frac{n(t)}{n_0}\right) + \frac{n_0}{N+n_0}\left(\frac{n(t)}{n_0}\right)^2\right) \qquad \text{(S3)}$$

where:

$$\frac{n(t)}{n_0} = \frac{e^{-At}}{1 + \frac{B}{A}\, n_0(1 - \, e^{-At})} \qquad \text{(S4)}$$

and:

$$I_0 = \gamma(N + n_0)n_0 \qquad \text{(S5)}$$

Here, I_0 is the initial PL intensity ($I_{PL}(t = 0)$), and γ is a constant that depends on factors such as the PL detection efficiency. By globally fitting the excitation power dependences of I_0 and the PL lifetime (Fig. S4) using eq. S3−S5, the values of *N, A*, and *B* are determined. The values of *A* and *B* are summarized in Table 2. The unintentional doped carrier density *N* is estimated to be 6.65×10^{13} cm^{-3} for PSCs before degradation and 3.46×10^{13} cm^{-3} after degradation.

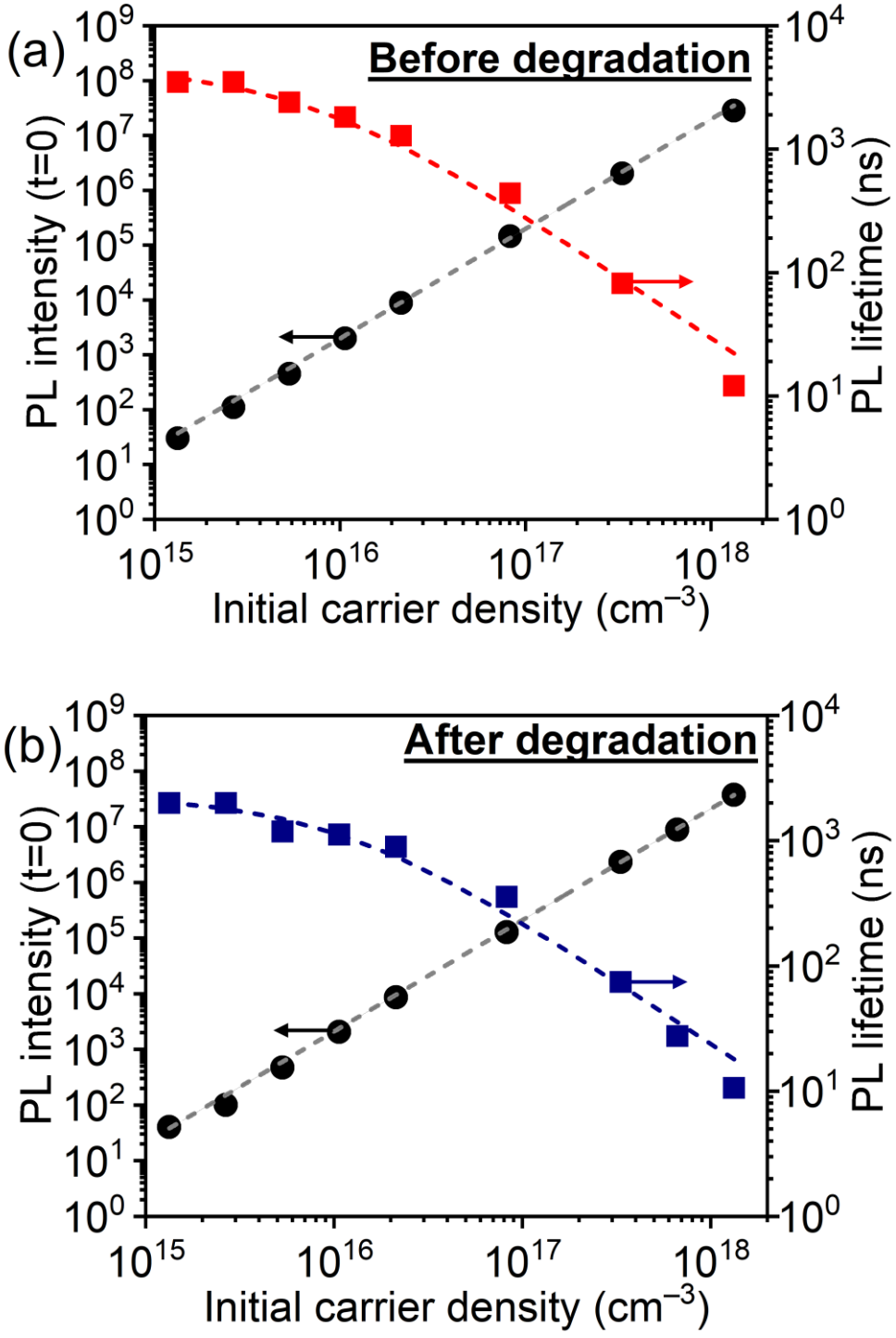

Fig. S4 Excitation power dependence on the initial PL intensity ($t = 0$) and the PL lifetime of perovskite monolayer samples of (a) before and (b) after thermal degradation. The dashed lines denote fitting curves.

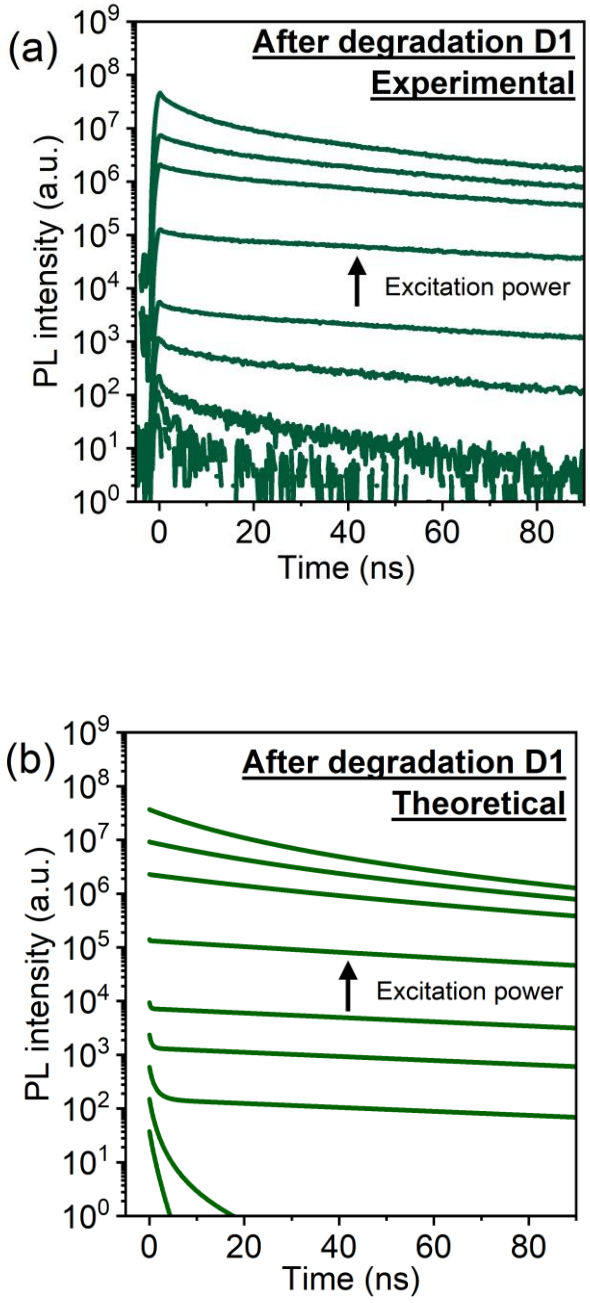

Fig. S5 Excitation power dependence on the PL decay (1–1000 nJ/pulse) of PSC after thermal degradation (D1 sample); (a) experimental and (b) theoretical results.

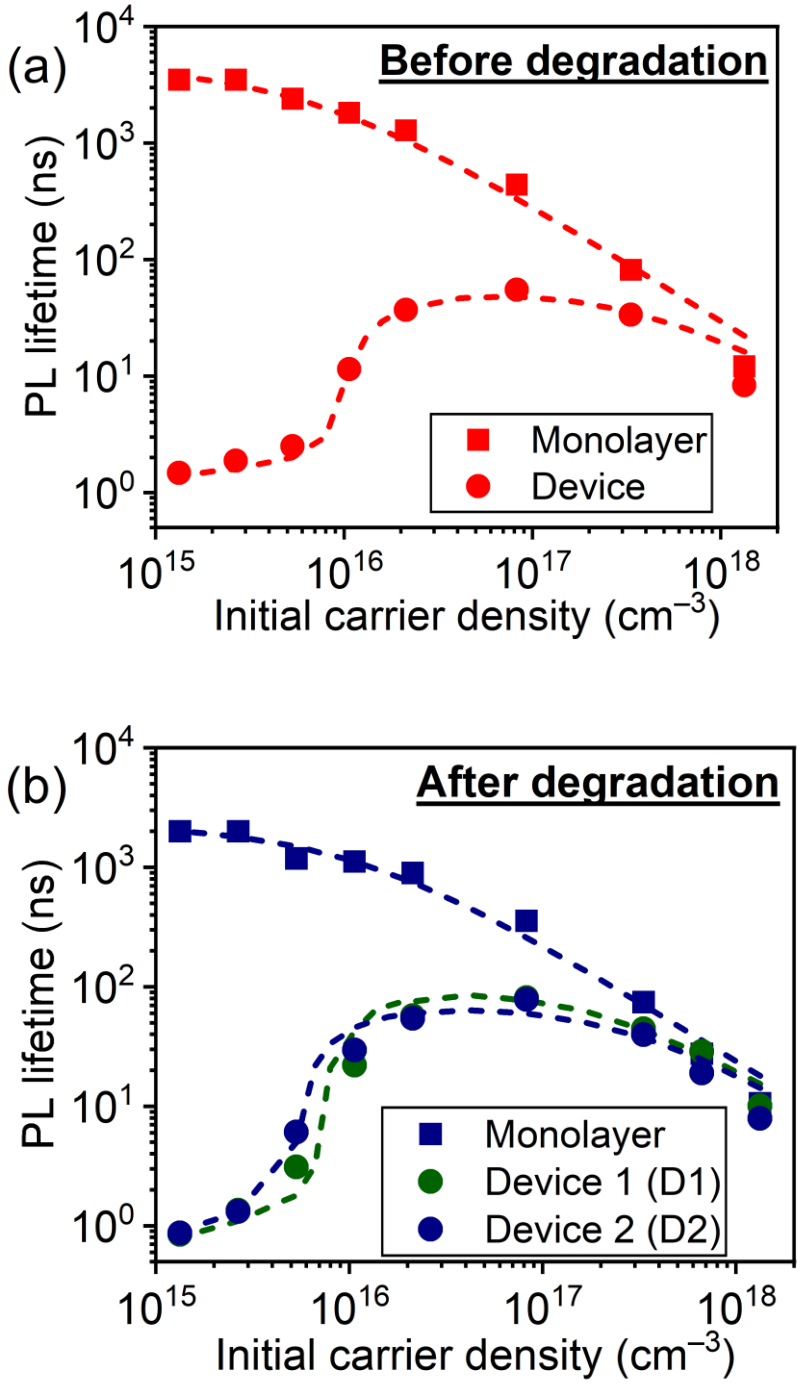

Fig. S6 Excitation power dependence (1–1000 nJ/pulse) of PL decay of solar cell device (dots) and monolayer (square) samples (a) before and (b) after degradation. The dot lines represent theoretical values. The initial photogenerated carrier density at 1 nJ/pulse corresponds to 1.33×10^{15} cm^{-3}.

3. Excitation intensity dependence on PV properties before and after thermal degradation

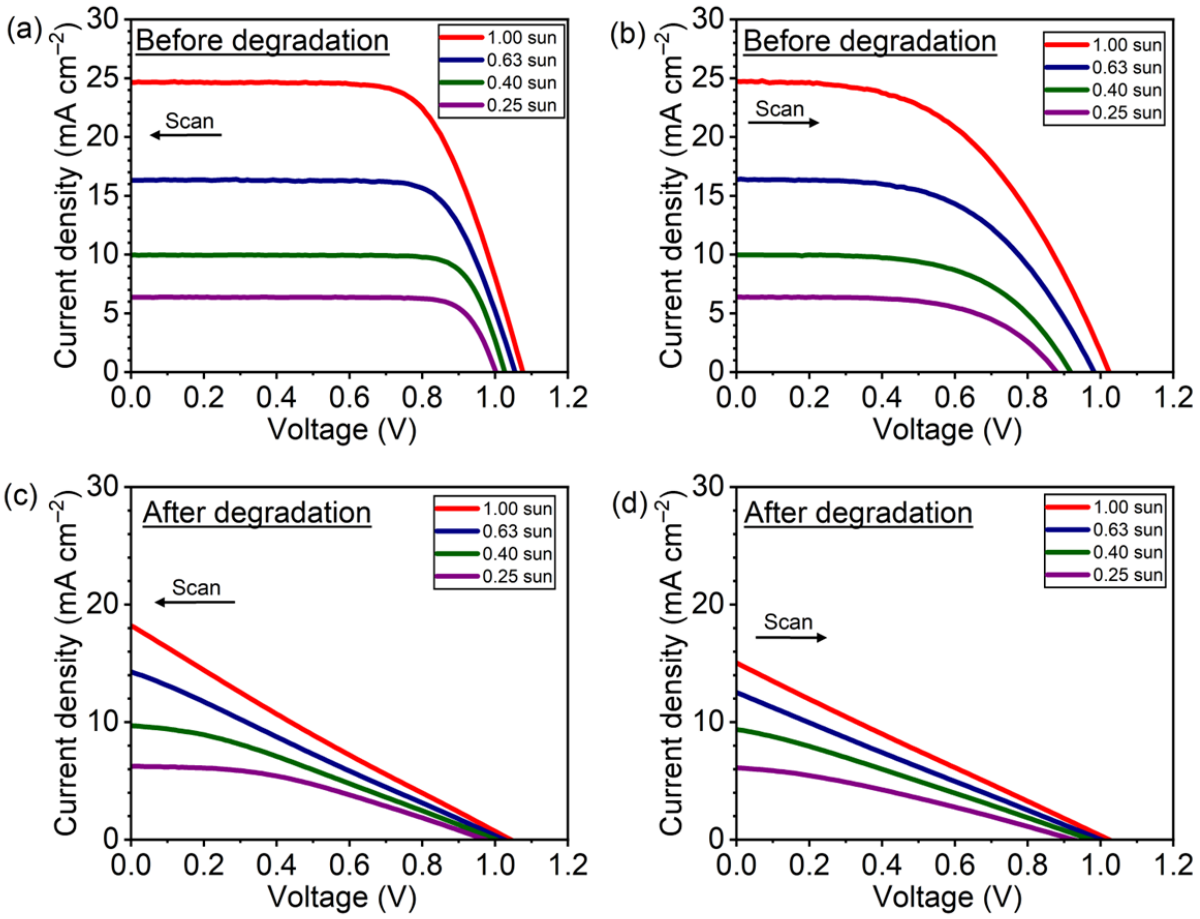

Fig. S7 Excitation intensity dependence on J-V curves of PSCs (a) before and (b) after thermal degradation.

Table S2. Excitation intensity dependence on PV parameters of PSCs (a) before and (b) after thermal degradation

(a)

Intensity (sun)	Scan	J_{sc} (mA/cm^{-2})	V_{oc} (V)	FF
1.00	Reverse	24.6	1.08	0.68
	Forward	24.7	1.02	0.50
0.63	Reverse	16.3	1.05	0.73
	Forward	16.4	0.98	0.54
0.40	Reverse	9.9	1.03	0.79
	Forward	10.0	0.92	0.58
0.25	Reverse	6.4	1.00	0.81
	Forward	6.4	0.88	0.59

(b)

Intensity (sun)	Scan	J_{sc} (mA/cm^{-2})	V_{oc} (V)	FF
1.00	Reverse	18.2	1.04	0.23
	Forward	15.0	1.02	0.25
0.63	Reverse	14.3	1.02	0.25
	Forward	12.5	1.00	0.25
0.40	Reverse	9.7	1.00	0.31
	Forward	9.4	0.97	0.27
0.25	Reverse	6.2	0.97	0.39
	Forward	6.1	0.93	0.31

Reference

1. T. Handa, D. M. Tex, A. Shimazaki, A. Wakamiya and Y. Kanemitsu, *J. Phys. Chem. Lett.*, 2017, **8**, 954-960.
2. N. Nishimura, R. K. Behera, R. Katoh, H. Kanda, T. N. Murakami and H. Matsuzaki, *J. Mater. Chem. C*, 2024, **12**, 9130-9138.
3. A. D. Wright, G. Volonakis, J. Borchert, C. L. Davies, F. Giustino, M. B. Johnston and L. M. Herz, *Nat. Mater.*, 2020, **19**, 1201-1206.